Image Mosaicing for Evaluation of MRI Brain Tissue Abnormalities Segmentation Study

Shafaf Ibrahim, Noor Elaiza Abdul Khalid, Mazani Manaf

***Abstract*—**Image segmentation and its performance evaluation are vital aspects in computer vision although they are challenging to resolve. Segmentation of Magnetic Resonance Imaging (MRI) brain images is essential to facilitate the neurological diseases diagnosis. Nevertheless, evaluation of segmentation accuracy has been fundamentally subjective that leads to difficulties in judging the effectiveness of the techniques implemented. This paper proposes an implementation of evaluation method known as image mosaicing in evaluating the MRI brain abnormalities segmentation study. Fifty seven mosaic images are formed by cutting various shapes and sizes of abnormalities, and pasting it onto normal brain tissues. The knowledge of pixel sizes of abnormalities is used as the ground truth to compare with various segmentation results. Three methods of Particle Swarm Optimization (PSO), Adaptive Network-based Fuzzy Inference System (ANFIS) and Fuzzy c-Means (FCM) are used to segment the mosaic images formed. The accuracies of image mosaicing segmentation are assessed using statistical analysis methods of Receiver Operating Characteristic (ROC) analysis. The statistical results obtained exhibit some variations that reflect the methods implemented. Thus, the proposed implementation of image mosaicing method is found to be acceptable as it produces potential solutions to the current difficulties of brain abnormalities segmentation performances evaluation.

***Keywords*—**Image mosaicing, Texture evaluation method, Medical imaging, Magnetic Resonance Imaging (MRI).

I. Introduction

IMAGE segmentation is one of the significant concerns in digital image processing. Yet, it has been broadly applied to various applications such as medical [1], multimedia [2], robotic [3] and database [4]. In recent years, segmentation has becoming a crucial stage in many medical imaging processing tasks for operation planning, radio therapy or diagnostics, and studying the differences of healthy subjects and subjects with tumor. Its purpose is to subdivide an image into meaningful non-overlapping regions which analysis, interpretation or quantification can be performed [5]. Up till now, it has been extensively investigated with a large number of image segmentation methods developed [1], [6]-[8]. Thus, reliable segmentation performance evaluation for quantitatively positioning the image segmentation is extremely important.

Evaluation is not only used in evaluating the performance of segmentation algorithms. It could also be used in combining the results of several segmentation results [9], and acted as a guide in selecting appropriate segmentation algorithms [10]. Nevertheless, evaluation of segmentation performance has been very subjective that leaves the researcher in tricky situation [11]. Therefore, it may leads to difficulties in judging the effectiveness of the techniques implemented. Chabrier *et al*. [12] found that it is difficult to evaluate the segmentation methods accuracy and efficiency on a single method as no one being optimal in all cases.

In many previous works, segmentation performance evaluation is divided into two categories of supervised and unsupervised methods [13]. In supervised method, the segmented images are compared and evaluated with a ground truth image which has been delineate by the experts. This method is claimed to be the best method because of its high evaluating accuracy [13]. Alternatively, unsupervised method does not require comparison with a manually segmented reference image [12] which the evaluation of segmentation is done visually.

From the reviews done, it is presumed that one of the biggest challenges in the medical imaging domain is to accurately and reliably quantify the clinical performance of the image processing algorithms and outcomes [38]. Up until now, loads of evaluation criteria have been proposed to quantify the quality of segmentation result [39], [40]. The common standard used for validating segmentation results of these segmentation methods is ground truth which the output of the segmentation may be compared [14], [15]. A main issue is that obtaining these validation data and comparison metrics for segmentation are difficult tasks due to the lack of reliable ground truth [16], [17]. Unfortunately, the lack of reliability and reproducibility of manual segmentation method should also be addressed [18]. Thus, even if a rich set of manual segmentations are available, they may not reflect the ground truth and the true gold standard may need to be estimated [19].

Manuscript received June 27, 2011: Revised version received August 11, 2011. This work was supported by the management of Research Management Institute (RMI), UiTM and financial support from E-Science Fund (06-01-01-SF0306) under the Minister of Science, Technology and Innovation (MOSTI), Malaysia.

Shafaf Ibrahim is with the Faculty of Computer and Mathematical Sciences, University Technology MARA, Shah Alam, Selangor, Malaysia, phone: 6019-2692717; fax: 604-5941023 (e-mail: shafaf_ibrahim@yahoo.com).

Noor Elaiza Abdul Khalid is with the Faculty of Computer and Mathematical Sciences, University Technology MARA, Shah Alam, Selangor, Malaysia. (e-mail: elaiza@tmsk.uitm.edu.my).

Mazani Manaf is with the Faculty of Computer and Mathematical Sciences, University Technology MARA, Shah Alam, Selangor, Malaysia (e-mail: mazani@tmsk.uitm.edu.my).

A segmentation outcome may vary, depending on the techniques employed and other constraints such as compactness. In some practice, the quality of a segmentation result is often visually assessed by the analyst. Despite of its simplicity and low cost, this method was claimed to be bias as the quality of the result relies on the experience of an analyst and lacks a quantitative support [20].

Another typical technique is the use of phantoms. For segmentation purpose, phantoms are usually synthetic images for which the true segmentation is known [21]-[23]. A physical object can also be used as a phantom ground truth where the phantom is measured and imaged. The original true measurement and segmentation measurements are then compared and performance is thus assessed [24]. However, for many medical problems, phantom studies are considered insufficient for validation and it is exceedingly difficult to design phantoms that appropriately imitate the living tissues [25].

Therefore, this study proposed an implementation of evaluation method which is known as image mosaicing. The image mosaicing method is used to generate synthetic ground truth of MRI images which exhibits comparable segmentation challenges to real MRI brain tissue abnormalities. The validation of the proposed image mosaicing for evaluation of brain abnormalities segmentation is then performed using three methods of Particle Swarm Optimization (PSO), Adaptive Network-based Fuzzy Inference System (ANFIS) and Fuzzy c-Means (FCM).

The organization of the rest of this paper is as follows: Section II presents our methods, including image mosaicing description, PSO, ANFIS and FCM algorithms structure. Section III discusses our results and discussions. Finally, we present our conclusion in Section IV.

II. Methods

Mosaicing of images have been in practice since the age of digital computers. Depending on its application, it is defined as the ability to combine groups of pictures with some overlapping areas. To date, image mosaicing strategy has been successfully employed in many research and application areas, as well as various representations of methods for image segmentation such as texture mapping [26], texture segmentation [27], edge detection [28], texturing three-dimensional modeling 29] and texture registration [30].

This paper emphasizes on the implementation of the image mosaicing method in solving one of the difficulties of MRI brain tissue abnormalities segmentation study. The method is implemented in evaluating the accuracy of segmentation performances.

A. *Image Mosaicing Formation*

The mosaic images are designed which that prior knowledge of size of abnormalities are known. This is done by cutting various shapes and sizes of brain abnormalities and pasting it onto normal brain tissues. The normal brain tissues are divided into three different categories of intensities. The process consists of three basic steps. The pictorial representation of the proposed mosaic image formation process is illustrated in Fig. 1.

1) Step 1: Background tissue selection
The background tissues are selected from normal area of brain tissue or so-called as membrane. These backgrounds are divided into three different categories of intensities which are “low”, “medium” and “high”, based on the grey level pixel value intensities as tabulated in Table I. The background images are cut into same size of pixels, as each of the background is vary in its minimum and maximum grey level pixel values. This is expected to show some significances and variances in analyzing the evaluation of segmentation outcome subsequently.

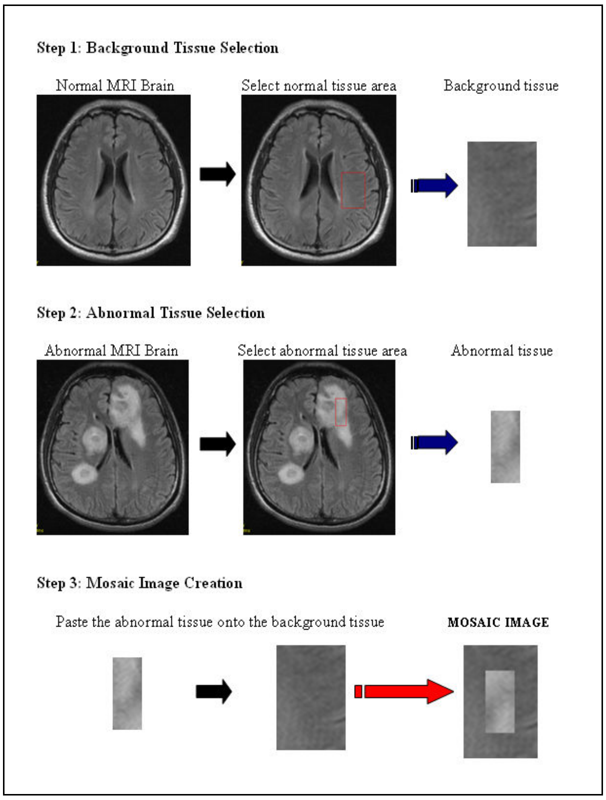

Fig. 1. Mosaic image formation process

Table I. Background Images

Background	**Intensity**	**Minimum grey level pixel value**	**Maximum grey level pixel value**	**Size in pixel**
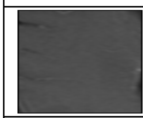	Low	30	114	12144
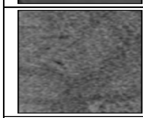	Medium	39	145	12144
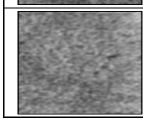	High	56	202	12144

2) Step 2: Abnormal tissue selection
The abnormal brain tissues are picked out from the abnormalities area which the sizes of abnormalities in pixels are known. Three possible shapes of selecting the abnormalities are square, oval or irregular shapes as illustrated in Table II. The differences in shapes of abnormalities selected may possibly contribute in discrepancy of segmentation performances.

Table II. Samples of Abnormalities Images

Shape	Image	Size in pixel
Square		1472
Oval	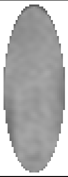	2010
Irregular	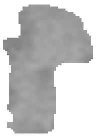	1901

3) Step 3: Paste the abnormal tissue onto the background tissue
Mosaic images are then formed by pasting the selected brain abnormality tissues onto the different background tissues as shown in Table III. This is used to test out the performances and level of accuracies of the segmentation outcome based on its combination of background intensity and shape of abnormalities.

Table III. Mosaic Images

Shape	Background Intensity		
	High	Medium	Low
Square	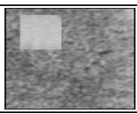	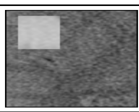	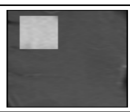
Oval	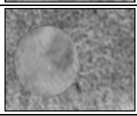	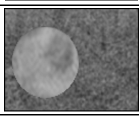	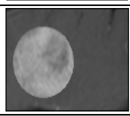
Irregular	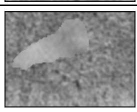	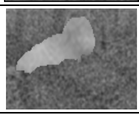	

B. Segmentation of Mosaic Images

After the process of mosaic images formation is completed, the segmentation of each mosaic image is performed. Three segmentation methods are used in this study which are Particle Swarm Optimization (PSO), Adaptive Network-based Fuzzy Inference System (ANFIS) and Fuzzy c-Means (FCM).

1) The Particle Swarm Optimization (PSO) Algorithm
PSO is an efficient search and optimization technique developed by Kennedy and Eberhart in 1995 [31]. The algorithm is based on a swarm of particles flying through the search space. In the concept of PSO, all individuals in the swarm have the same characteristics and behaviours, and each individual contains parameters for position and velocity. The position of each particle represents a potential solution to the optimization problem. The velocity is governed by a set of rules that control the dynamics of the swarm. In order to apply the PSO idea, matters such as representation of initial population, representation of position and velocity strategies, fitness function identification and the limitation should first be considered. In the proposed PSO algorithm the four essential parameters that are considered are as tabulated in Table IV.

Table IV. PSO Parameters

Parameters	Description
Particle	candidate solution to a problem
Velocity	rate of position change
Fitness	the best solution achieved
pbest	best value obtained in previous particle

The proposed PSO consist of four main steps that is the initial generation swarm of particles, fitness function examination, position and velocity update and finally the termination criterion determination. The pictorial representation of the proposed PSO processes is illustrated in Fig. 2.

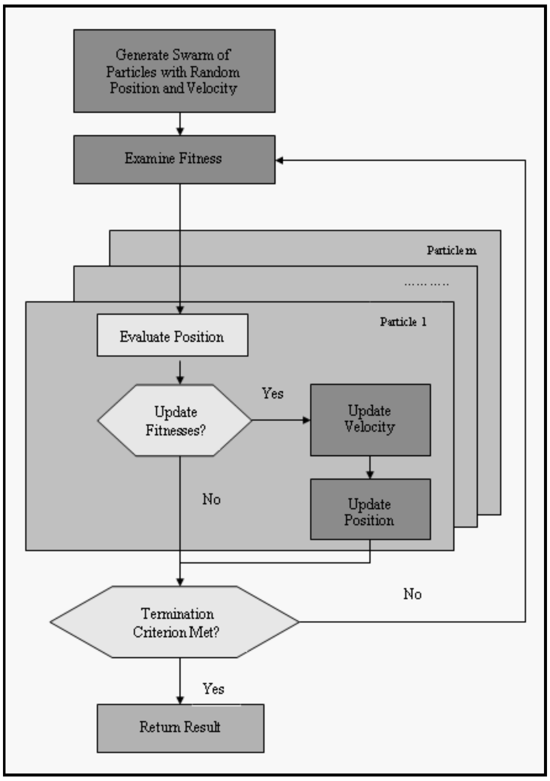

Fig. 2. Proposed PSO Processes

a) Generation of Particles
The initial swarm particles proposed PSO is initialized to contain 400 points of particles with random position and velocity. The points had been randomly selected in the X-axis value within the image width while the Y-axis value within the image height.

b) Fitness Examination
Each particle's fitness are then examined with the fitness function based on the minimum, maximum and mean grey level pixel value of the ventricles, membrane, light abnormality and dark abnormality. A particular particle is considered as fit (*pbest*) if and only if it matches all these three values. Otherwise, the particle will be automatically ignored and removed.

c) Position and Velocity Update
Velocity depends on the rate of position change of the particle's position. The position and velocity in the proposed algorithm is set as the four neighbouring pixels of particle at (x,y) shown in Fig. 3. The coordinates of the neighbouring pixels are (x, y-1), (x-1, y), (x, y+1) and (x+1, y). This process is done iteratively on the particles of the swarm and fitted particles are stored as the personal current best (*pbest*). The iteration of updated rules of position and velocity leads to the exploration of the whole regions that turn out to be the final outcomes.

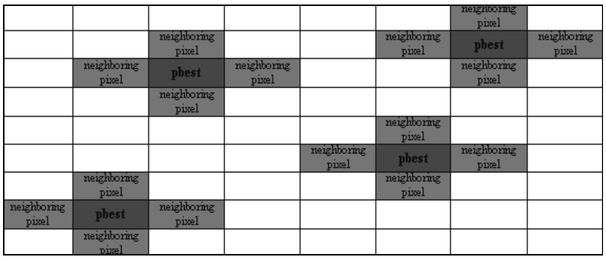

Fig. 3. Proposed Principle of Updating Velocity

The maximum velocity is limited to the whole region of each MRI brain images. It is chosen for facilitating global exploration of particle's position since too low maximum velocity region might leads the difficulties of particles in exploring the optimal regions.

d) Termination Criterion Determination
The proposed technique termination criterion processes of fitness examination, velocity and position update are performed iteratively until the termination criterion is met. Therefore, the process will stop and return the result when there are no unprocessed *pbest* pixels in the maximum velocity regions. Otherwise, the process will continue to iterate the fitness examination, velocity and position update processes for the next particles.

2) Adaptive Network-based Fuzzy Inference System (ANFIS) Algorithm
ANFIS is implementation with fuzzy inference system in the framework of adaptive network. ANFIS architecture cans employs to model non linear function, identify nonlinear components in a control system and expect a chaotic time series [32].
The objective of ANFIS is to integrate the best features of Fuzzy System and Neural Networks. Fig. 4 shows the ANFIS architecture that has 5 layers.

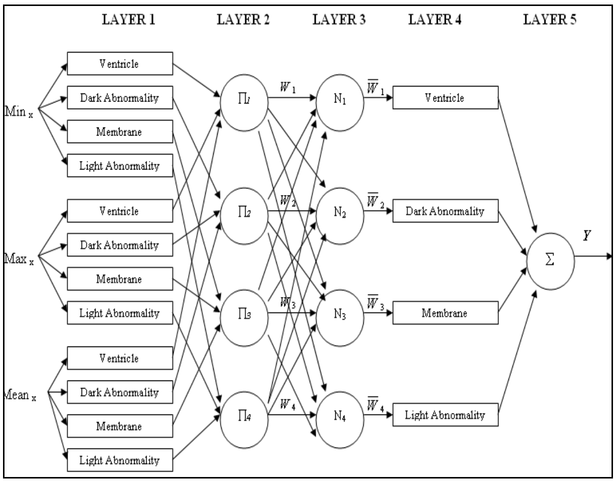

Fig. 4. Proposed ANFIS architecture

In the first layer, all the nodes are adaptive nodes. The outputs of layer 1 are the fuzzy membership grade of the inputs, which are:

$$o_i^1 = \pi A_i(x) \quad (1)$$

Where x is the input to node i and A_i is a linguistic label such as minimum, maximum and mean grey level value associated with the node. o_i^1 is the membership function of A_i and it specifies the degree to which the given x satisfies the quantifier A_i. $\pi A_i(x)$ is triangle-shaped Membership Function (MF) value ranging from 0 to 1 such as:

$$\pi A_i(x) = \frac{1}{1+(x-c_i/a_i)^{2bi}} \quad (2)$$

where a_i, b_i and c_i are the parameters of the membership function, governing the triangle-shaped function accordingly.

In the second layer, the nodes are fixed nodes. Each node in this layer represents firing strength of the rules. They are labeled with π, indicating that perform as a simple multiplier. The outputs of this layer can be represented as:

$$o_i^2 = w_i = \pi A_i(x_1) \times \pi B_i(x_2) \times \pi C_i(x_3) \ldots \quad (3)$$

where

i = 1, 2, 3…..n

$x_1, x_2, x_{3 \ldots n}$ = input

O_i^2 = output of neuron i.

In the third layer, the nodes are also fixed nodes labeled by N, to indicate that they play a normalization role to the firing strength from the previous layer. The output of this layer can be represented as:

$$o_i^3 = \overline{w_i} = \frac{w_i}{w_1 + w_2 + w_3 + w_4} \quad (4)$$

In the forth layer, the nodes are adaptive. The output of each node in this layer is simply the product of the normalized firing strength and a first order polynomial. Thus, the output of this layer is given by:

$$o_i^4 = \overline{w_i} f_i = \overline{w_i}(p_i x_1) + q_i x_2 + r_i x_3 + s_i) \quad (5)$$

Where $\overline{w_i}$ is the output of layer 3 and p_i, q_i and r_i is the parameter set. Parameter in this layer will be referred to as consequent parameters.

In fifth layer, the single layer node is a circle node labeled ∑ that computes the overall output as the summation of all incoming signal such as:

$$o_i^5 = \sum \overline{w_i} f_i \quad (6)$$

3) Fuzzy c-Means (FCM) Algorithm

FCM is an iterative algorithm that aims to find cluster centers in an image that minimizes an objective function. A process called as fuzzy partitioning is employed which a data point can belong to all groups with different membership grades between 0 and 1 [20]. The objective function is the sum of squares distance between each pixel and the cluster centers and is weighted by its membership. FCM is defined by six parameters which are shown in Table V.

Table V. Parameters for FCM Algorithm

Parameters	Description
n	number of data samples for whole images
c	number of clusters
x_k	k_{th} data sample (Pixel point value)
v_i	i_{th} cluster center
m	weighting exponent (constant greater than unity)
μ_{ki}	membership of x_k in i_{th} cluster

Step 1: Initialize the constants c, m and ε such that:

$1 \leq c \leq n$

$1 \leq m \leq \infty$

$\varepsilon \geq 0$ a small positive constant

Step 2: Initialize the cluster centers:

$$V_0 = (v_{1.0}, v_{2.0} \ldots v_{c.0}) \in R^{CP}$$

For our FCM implementation, the image was clustered into two, which represent abnormality and background based on features values. The algorithm starts by initializing cluster centers to a random value at first time. The performance depends on the initial clusters, thereby allowing running FCM several times, each starting with a different set of initial clusters.

Step 3: Update the membership values, μ_{ki} using (7):

$$u_{ki} = \frac{1}{\sum_{j=1}^{c}\left(\frac{\|x_k - v_i\|}{\|x_k - v_j\|}\right)^{2/(m-1)}} \quad (7)$$

Different values of may produce different segmentation results. Based on literature, the value weighting exponent, m = 2 was used, to get good performance of FCM.

Step 4: Update the cluster centers, v_i using (8):

$$v_i = \frac{\sum_{k=1}^{n} (\mu_{ik})^m x_k}{\sum_{k=1}^{n} (\mu_{ik})^m} \qquad (8)$$

Step 5: Check terminating condition, E_t using (9):

$$\text{Let} \qquad E_t = \sum_{i=1}^{n} \left\| v_{i,t} - v_{i,t-1} \right\|^2 \qquad (9)$$

This process is repeated until terminating condition, E_t is below a certain stopping criteria. Else, repeat step 3 to step 5.

C. Evaluation of Image Mosaicing Segmentation

Receiver Operating Characteristic (ROC) statistical method of analysis is employed to quantify the segmentation accuracy of image mosaicing. ROC analysis is a plot of the true positive fraction versus the true negative fraction that produced by classifying each data point as positive and negative according to outcome [33] It has been effectively used as a statistical validation tools in various areas of segmentation such as mammograms [34], retinal [35], brain [36] and skin [37].

In this paper, the numbers of pixels of the raw MRI brain images are compared with the segmented abnormality area of mosaic images. ROC is used to measure the value of false positive, false negative, true positive and true negative. Four conditions areas of false positive, false negative, true positive and true negative are illustrates in Fig.5.

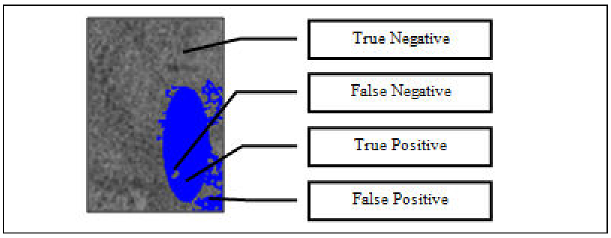

Fig. 5. Sample of mosaic image of Oval Abnormality within Medium Background intensity after segmentation

The four primary conditions are used as tools in identifying the PSO, ANFIS and FCM segmentation qualities and the level of accuracies. The descriptions and states for each condition are explained in Table VI.

Table VI. Conditions of Accuracy

Condition	Description	State	Calculation
False Positive	normal areas that are incorrectly detected as abnormality	If segmented area > abnormality area	(segmented area - abnormality area) / background size in pixels
		If segmented area <= abnormality area	0
False Negative	abnormality areas that are not detected	If segmented area >= abnormality area	0
		If segmented area < abnormality area	(abnormality area - segmented area) / background size in pixels
True Positive	abnormality areas that are correctly detected	If segmented area >= abnormality area	1
		If segmented area < abnormality area	1 - (abnormality area - segmented area) / background size in pixels
True Negative	normal areas that are correctly undetected	If segmented area > abnormality area	1 - (segmented area - abnormality area) / background size in pixels
		If segmented area <= abnormality area	1

III. Results and Discussion

The numbers of pixels of the raw MRI brain images are compared with the segmented abnormality area of mosaic images. The segmentation accuracy results are then measured by analysing the ROC values of false positive, false negative, true positive and true negative.

Table VII shows a few samples of segmentation outcomes tested to square, oval and irregular shapes of light and dark abnormalities onto the high, medium and low background tissue intensities.

Table VII. PSO vs ANFIS vs FCM Segmentation

Shape	B/Ground Intensity	Mosaic Image	PSO	ANFIS	FCM
Square	High	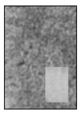	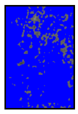	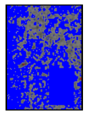	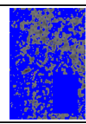
	Medium	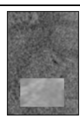	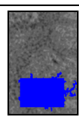	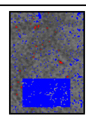	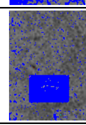
	Low		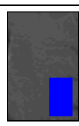	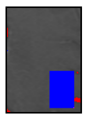	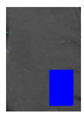
Oval	High	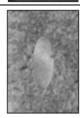	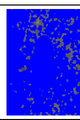	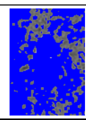	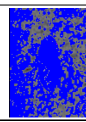
	Medium	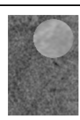	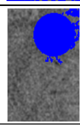	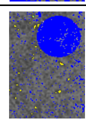	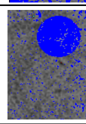

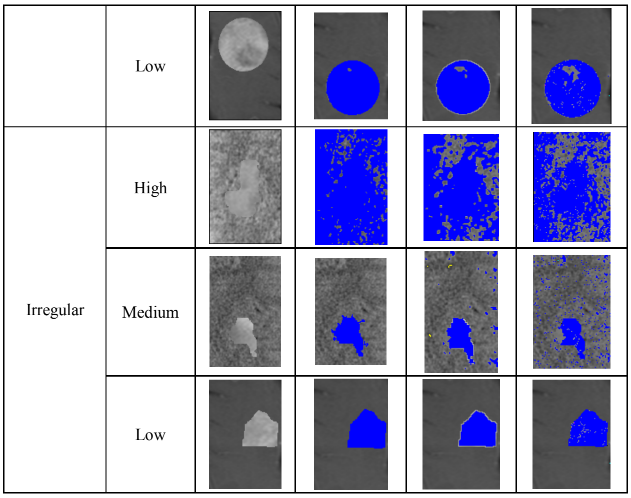

Three techniques had been chosen for the segmentation of fifty seven mosaic images which are PSO, ANFIS and FCM. Then, every mean value of false positive, false negative, true positive and true negative is evaluated by relating the results to any certain circumstances. Table VIII, Table IX and Table X tabulate the summary of ROC analysis for PSO, ANFIS and FCM segmentation results which includes the entire four primary conditions.

Table VIII. Summary of ROC Analysis for PSO

Shape	**B/Groun d Intensity**	**Mean of False Positive**	**Mean of False Negative**	**Mean of True Positive**	**Mean of True Negative**
Square	High	0.569	0	1	0.431
	Medium	0.008	0.001	0.999	0.992
	Low	0	0.004	0.996	1
Oval	High	0.535	0	1	0.465
	Medium	0	0.003	0.997	1
	Low	0	0.055	0.945	1
Irregular	High	0.642	0	1	0.358
	Medium	0.003	0	1	0.997
	Low	0	0.016	0.984	1

As seen from the Table VIII, PSO shows the most excellent segmentation result in low background intensity for square and oval shapes. The statistics show that the combination of abnormality within the low background intensity value produced the highest mean percentages for both true positive and true negative which are the most important condition in producing good quality of segmentation. This proved that the PSO segmentation results of the mosaic images showed some potential as the mean values of false positive and false negative are kept at a very low rate too. The combination of abnormality within the medium background intensity also cannot be underestimated since it produced high mean values for both true positive and true negative. However, small occurrence of false positive is observed. The irregular produced most optimum segmentation result in medium background intensity followed by low and high background intensities respectively. The combination of abnormality within the high background intensity is seen to produce poor performance regardless of any shapes of abnormalities as it appears the highest mean value of false positive compared to the medium and low background intensities. This is found to be caused by the texture similarity for both abnormality and high background intensity that leads the neighboring pixels to grow beyond the abnormality areas.

Table IX. Summary of ROC Analysis for ANFIS

Shape	**B/Groun d Intensity**	**Mean of False Positiv e**	**Mean of False Negativ e**	**Mean of True Positiv e**	**Mean of True Negativ e**
Square	High	0.642	0	1	0.358
	Medium	0.009	0.044	0.956	0.991
	Low	0	0.194	0.806	1
Oval	High	0.628	0	1	0.372
	Medium	0.005	0.056	0.944	0.995
	Low	0	0.198	0.802	1
Irregular	High	0.647	0	1	0.353
	Medium	0.008	0.051	0.949	0.992
	Low	0	0.179	0.821	1

The ANFIS is observed to produce an optimum segmentation of abnormality in medium background intensity as it produced the highest mean values for both true positive and true negative in all three shapes of square, oval and irregular. The performance of abnormality segmentation in low background intensity also returns good segmentation outcome as it displays excellent mean value of true negative in all shapes. However, there is slightly lower in the mean of true positive value since it is affected by the small occurrence of false negative. Same as PSO, the segmentation of abnormality within the high background intensity performed unsatisfactorily since it produced the highest mean value of false positive compared to the medium and low background intensities. In the context of different shapes of abnormality selection, the results of ANFIS segmentations show some distinction as the oval is found to produce the most accurate segmentation outcomes generally regardless of background as compared to square and irregular.

Table X. Summary of ROC Analysis for FCM

Shape	**B/Groun d Intensity**	**Mean of False Positiv e**	**Mean of False Negativ e**	**Mean of True Positiv e**	**Mean of True Negativ e**
Square	High	0.566	0	1	0.434
	Medium	0.050	0	1	0.950
	Low	0	0.043	0.957	1
Oval	High	0.545	0	1	0.455
	Medium	0.037	0.004	0.996	0.963
	Low	0	0.073	0.927	1
Irregular	High	0.572	0	1	0.428
	Medium	0.052	0	1	0.948
	Low	0.001	0.021	0.979	0.999

Alternatively, FCM returns almost the same outcomes as PSO where it produced a most excellent performance of segmentation in low background intensity since it keeps the mean values for both true positive and true negative at the highest assessment. The combination of abnormality within the medium background intensity also cannot be underrated since it produced high mean values for both true positive and true negative in all square, oval and irregular shapes. However, small occurrence of false positive and false negative are monitored. The combination of abnormality within the high background intensity exhibits poor performance by returning the highest value of false positive despite of background intensities and abnormality shapes.

The second analysis method employed is Pearson's correlation. Pearson's correlation is widely used to reflect the degree of linear relationship between two variables. In this paper, the Pearson correlation value of three categories between the original abnormalities area vs PSO, original abnormalities area vs ANFIS, and original abnormalities area vs FCM segmentation pixels value are measured so that the variation of results obtained can be clearly monitored. The Pearson's correlation value for each categories mentioned is presented in Table XI:

Table XI. Pearson's correlation for PSO, ANFIS and FCM

Description	B/Ground	Correlation value
Original vs PSO Correlation	High	0.872
	Medium	0.993
	Low	0.999
Original vs ANFIS Correlation	High	0.894
	Medium	0.999
	Low	0.999
Original vs FCM Correlation	High	0.927
	Medium	0.998
	Low	0.507

From the table above, it clearly noticed that PSO and ANFIS correlation values are almost excellent in abnormalities segmentation regardless of background. However, the correlation values of the FCM shows a slightly lower value in low background tissue intensity.

IV. Conclusion

This paper proposed an implementation of image mosaicing as an evaluation method for brain tissue segmentation study. The application to a variety of MRI brain medical data has been successful. The techniques of Particle Swarm Optimization (PSO), Adaptive Network-based Fuzzy Inference System (ANFIS) and Fuzzy c-Means (FCM) had been tested for the evaluation as well as quantification of the image mosaicing segmentation. The results obtained exhibit some variations that reflect the techniques implemented. Therefore, it can be conclude that the proposed implementation of image mosaicing as an evaluation method is found to be reasonable and acceptable to use as it produces potential solutions to the current difficulties in evaluating and validating the brain tissue abnormalities segmentation outcome.

Acknowledgment

The authors acknowledge with gratitude the great support from the management of Research Management Institute (RMI), UiTM and financial support from E-Science Fund (06-01-01-SF0306) under the Minister of Science, Technology and Innovation (MOSTI), Malaysia.

References

[1] S. Ibrahim, N.E.A Khalid, and M. Manaf, "Empirical Study of Brain Segmentation using Particle Swarm Optimization", *International Conference on Information Retrieval and Knowledge Management*, CAMP'10, pp. 235-239, 2010.

[2] N. Ikonomakis, K.N. Plataniotis, and A.N. Venetsanopoulos, "Color Image Segmentation for Multimedia Applications", *Journal of Intelligent & Robotic Systems*, Vol. 28, No. 1-2, June, 2000, pp. 5-20, 2000.

[3] T. Kubik, and M. Sugisaka, "Image segmentation techniques and their use in artificial life robot implementation", *Journal of Artificial Life and Robotics*, Vol. 7, No. 1-2, March, 2003, pp. 12-15, 2003.

[4] A.L. Ratan, O. Maron, W.E.L Grimson, and T. Lozano-Perez, "A framework for learning query concepts in image classification", *Proceedings of the IEEE Conference on Computer Vision and Pattern Recognition*, pp. 423-431, 1999.

[5] I.V.Gribkov, P.P.Koltsov, N.V.Kotovich, A.A. Kravchenko, A.S.Koutsaev, A.S. Osipov, A.V. Zakharov, "Comparative Study of Image Segmentation Algorithms", *8th WSEAS International Conference On Signal, Speech And Image Processing* (SSIP '08), Santander, Cantabria, Spain, September 23-25, pp. 21-28, 2008.

[6] Jeng-Ming Yih, Yuan-Horng Lin, Hsiang-Chuan Liu, "Clustering Analysis Method Based on Fuzzy c-Means Algorithm of PSO and PPSO with Application in Image Data", *Proceedings of The 8th WSEAS International Conference on Applied Computer Science* (Acs'08), Pp. 54-59, 2008.

[7] Eko Supriyanto, Mohd Aminudin Jamlos, Lim Khim Kheung, "Segmentation of Carotid Artery Wall Towards Early Detection of Alzheimer Disease", *15th WSEAS International Conference on Computers*, Corfu Island, Greece, July 15-17, Pp. 201-206, 2011.

[8] N.E.A. Khalid, S. Ibrahim, M. Manaf, and U.K. Ngah, "Seed-Based Region Growing Study for Brain Abnormalities Segmentation", *International Symposium on Information Technology 2010 (ITSim 2010)*, Vol. 2, pp. 856 - 860 2010.

[9] C. Reosenberger, and K. Chehdi, "Genetic Fusion: Application to Multi-components Image Segmentation", *Proceedings ICASSP*, 4: pp. 2223-2226, 2000.

[10] Y.J. Zhang, and H.T. Luo, "Optimal Selection of Image Segmentation Algorithms based on Performance Evaluation", Optical Engineering, Vol. 39, Issue 6, pp. 1450-1456, 2000.

[11] R. Unnikrishnan, C. Pantofaru, and M. Hebert, "A Measure for Objective Evaluation of Image Segmentation Algorithms", *Workshop on Empirical Evaluation Methods in Computer Vision*, *IEEE Conference on Computer Vision and Pattern Recognition (CVPR '05)*, June 2005, 2005.

[12] S. Chabrier, H. Lauren, and B. Emile, "Performance Evaluation of Image Segmentation Application to Parameters Fitting", *Proceedings of European Signal Processing*, 2005.

[13] J.A. Koupaei, and M. Abdechiri, M., "An Optimization Problem for Evaluation of Image Segmentation Methods", *International Journal of Computer and Network Security (IJCNS),* Vol. 2, No. 6, June 2010, 2010.

[14] V. Grau, A.U.J. Mewes, M. Alcaniz, R. Kikinis, and S.K. Warfield, "Improved watershed transform for medical image segmentation using prior information", *IEEE Trans. Med. Imag. 23 (4),* pp. 447-458, 2004.

[15] D.E. Rex, D.W. Shattuck, R.P. Woods, K.L. Narr, E. Luders, K. Rehm, S.E Stolzner, D.A. Rottenberg, and A.W. Toga, "A meta-algorithm for brain extraction in MRI", *NeuroImage 23*, pp. 625-627, 2004.

[16] M. Prastawa, E. Bullita, and G. Gerig," Simulation of Brain Tumors in MR Images for Evaluation of Segmentation Efficacy", *Medical Image Analysis*, 2009 – Elsevier, Vol. 13, Issue 2, April 2009, pp. 29-311, 2009.

[17] X. Lin, T. Qiu, F. Nicolier, and S. Ruan, "Automatic Hippocampus Segmentation from Brain MRI Images", *International Journal of Computer Information Systems and Industrial Management Applications*, Vol. 2, pp. 1-10, 2010.

[18] A.P. Zijdenbos, R. Forghani, and A.C. Evans, "Automatic "pipeline" analysis of 3-D MRI data for clinical trials: application to multiple sclerosis", IEEE *Trans. Med. Imag. 21 (10),* pp. 1280-1291, 2002.

[19] S.K. Warfield, K.H. Zou, and W.M. Wells, "Simultaneous truth and performance level estimation (STAPLE): an algorithm for the validation of image segmentation", *IEEE Trans. Med. Imaging 23 (7),* pp. 903-921, 2004.

[20] H. Zhu, and H. Chen, "A Quantitative Evaluation of Image Segmentation Quality", ASPRS *2009 Annual Conference*, Maryland, March 8-13, 2009.

[21] D.L. Collins, A.P. Zijdenbos, V. Kollokian, J.G. Sled, N.J. Abani, C.J. Holmes, and A.C. Evans," Design and construction of a realistic digital brain phantom", *IEEE Trans. Med. Imag. 17 (3),* pp. 463-468, 1998.

[22] Y. Zhang, M. Brady, and S. Smith, "Segmentation of brain MR images through a hidden Markov random field model and the expectation maximization algorithm", *IEEE Trans. Med. Imag. 20 (1)*, pp.45-57, 2001.

[23] J. Ashburner, and K. Friston, "Spatial normalization using basis functions", In: R.S.J. Frackowiak, K.J. Friston, C. Frith, R. Dolan, K.J. Friston, C.J. Price, S. Zeki, J. Ashburner, and W. Penny, (Eds.), *Human Brain Function*, 2nd edition, Academic Press, 2003.

[24] J.D. Klingensmith, R. Shekhar, and D.G. Vince, "Evaluation of threedimensional segmentation algorithms for the identification of luminal and medial–adventitial borders in intravascular ultrasound images", *IEEE Trans. Med. Imag. 19 (10)*, pp. 996-1011, 2000.

[25] S. Bouix, M. Martin-Fernandez, L. Ungar, M. Nakamura, M. Koo, R. McCarley, and M. Shenton, "On evaluating brain tissue classifiers without a ground truth", *Neuroimage* 07, 447458, 2007.

[26] S.L. Victor, and V.I. Denis, V.I., "Seamless Mosaicing of Image-Based Texture Maps", *IEEE Computer Society Conference on Computer Vision and Pattern Recognition*, 2007.

[27] T. Hofmann, J. Puzicha, and J.M. Buhmann, "An Optimization Approach to Un-supervised Hierarchical Texture Segmentation". *ICIP*, 1997.

[28] L. Wolf, X. Huang, I. Martin, and D. Metaxas, "Patch-Based Texture Edges and Segmentation", *Proceedings of the European Conference on Computer Vision (ECCV)*, May 2006.

[29] A. Baumberg, "Blending Images for Texturing 3D Models", *Proceedings of the British Machine Vision Conference (BMVC)*, 2002.

[30] H. Lensch, W. Heidrich, and H. Seidel, "A Silhouette-Based Algorithm for Texture Registration and Stitching". *Journal of Graphical Models*, Vol. 63, No. 4, pp. 245-262, 2001.

[31] Kennedy J., Eberhart R., "Particle Swarm Optimization", *In Proceedings of IEEE International Conference on Neural Networks*, 1995, pp.1942-1948.

[32] J.S.R. Jang, "ANFIS: Adaptive-Network-Based Fuzzy Inference System", *IEEE Transactions on Systems, Man, And Cybernetics*, Vol. 23, No. 3, May-june 1993, pp. 665-685, 1993.

[33] M. Gribskov, and N.L. Robinson, "Use of receiver operating characteristic (ROC) analysis to evaluate sequence matching", *Comput. Chem.,* Vol. 20(1), pp. 25-33, 1996.

[34] W. Qian, L. Li, and L.P. Clarke, "Image feature extraction for mass detection in digital mammography: Influence of wavelet analysis", *The International Journal of Medical Physisc Research and Practice*, Vol. 26, Issue 3, 1999.

[35] V.B.S. Joao, J.G.L. Jorge, M.C. Roberto Jr., F.J. Herbert, and J.C. Michael, "Retinal Vessel Segmentation Using the 2-D Morlet Wavelet and Supervised Classification", *Journal of IEEE Trans Medical Imaging*, Vol. 25, no. 9, pp. 1214-1222, Sep. 2006.

[36] M.D. Budde, J.H. Kim, H.F. Liang, R.E. Schmidt, J.H. Russell, A.H. Cross, and S.K. Song, "Toward accurate diagnosis of white matter pathology using diffusion tensor imaging", *Journal of Magnetic Resonance in Medicine*, Vol. 57, Issue 4, pp. 688-695, April 2007.

[37] L. Sigal, S. Sclaroff, and V. Athitsos, "Skin color-based video segmentation under time-varying illumination", *IEEE Transactions on Pattern Analysis and Machine Intelligence*, Vol. 26, Issue 7, pp. 862-877, July 2004.

[38] Chi-Man Pun and Hong-Min Zhu, "Textural Image Segmentation Using Discrete Cosine Transform", *Proceedings of the 3rd International Conference on Communications and Information Technology* (Cit '09), Vouliagmeni, Athens, Greece December 29-31, pp. 54-58, 2009.

[39] Shafaf Ibrahim, Noor Elaiza Abdul Khalid, Mazani Manaf, "Evaluation Method for MRI Brain Tissue Abnormalities Segmentation Study*", 15th WSEAS International Conference on Computers*, Corfu Island, Greece, July 15-17, pp. 297-302, 2011.

[40] Noor Elaiza Abdul Khalid, Shafaf Ibrahim, Mazani Manaf, "Brain Abnormalities Segmentation Performances Contrasting: Adaptive Network-Based Fuzzy Inference System (ANFIS) vs K-Nearest Neighbors (k-NN) vs Fuzzy c-Means (FCM)*", 15th WSEAS International Conference on Computers*, Corfu Island, Greece, July 15-17, pp. 285-290, 2011.

Shafaf Ibrahim is a third semester student of PhD in Science in University Technology MARA, Shah Alam, Malaysia. She holds a Master in Computer Science (2009) and a Bachelor's Degree of Computer Science (2007), all from University Technology MARA. Her research interest covers Image Processing, Medical Imaging, Computer Vision, Artificial Intelligence and Swarm Intelligence.

Dr Noor Elaiza Abdul Khalid is a lecturer in University Technology MARA, Shah Alam, Malaysia. She holds a PhD in Computer Science (2010) from University Technology MARA, a Master in Computer Science (1992) from University of Wales and a Bachelor's Degree of Computer Science (1995) from University Science Malaysia. Her research interests are Swarm Intelligence, Evolutionary Computing algorithms**,** Fuzzy and Medical Imaging.

Assoc. Prof. Dr. Mazani Manaf is a lecturer in University Technology MARA, Shah Alam, Malaysia. He holds respected position at Faculty of Computer Science and Mathematics as Deputy Dean (Student & Alumni), with various professional and community activities and program assessor. His research interest covers Image Processing, Pattern Recognition & Machine Intelligent and Mobile & Distributed Computing.